MODELLING OF SHADOWING LOSS DUE TO HUGE NON-POLYGONAL STRUCTURES IN URBAN RADIO PROPAGATION

A. Kara [†]

Atilim University
Department of Electrical and Electronics Engineering
Incek, Ankara, Turkey

E. Yazgan

Hacettepe University
Department of Electrical and Electronics Engineering
Beytepe, Ankara, Turkey

Abstract—Ray tracing algorithms rely on two dimensional or three dimensional database. They use ray optical techniques referred to as the uniform theory of diffraction (UTD) using building database given as polygons. Building geometries can also be modelled as having non-planar geometries, and this would be important in modeling of shadowing loss due to curved structures in urban radio propagation. To demonstrate modelling of buildings as non-polygonal geometries, a particular building composition involving 3D cruved geometries is chosen, and shadowing loss for this building composition is studied via UTD ray tracing. Building structure considered in this study involves main canonical shapes of non-planar geometries including cone, cylinder and sphere. Single and multiple interaction of surface diffractions, effect of creeping waves are taken into consideration in the analysis.

[†] Also with TUBITAK, UEKAE/G222 Ataturk Bulvari, No:211, Kat:7/20, Kavaklidere, Ankara, Turkey

1. INTRODUCTION

Ray tracing algorithms have usually been used to model the radio propagation in high-rise core, the urban environment, of the city. They predict not only amplitude of received signal level for coverage and interference evaluation but also time of arrival (TAO) and delay spread, direction of arrival (DOA) and many other operational parameters of a system prior to deployment [1]. Depending on the type of the environment and capability of algorithms, ray tracing algorithms rely on two dimensional or three dimensional database of a region [1]. That the buildings are modelled as polygonal in vertical and horizontal plane simplifies a complex structure to a simpler one. In determining signal level at a receiver location, ray tracing codes have used ray optical techniques referred to as the Uniform Theory of Diffraction (UTD) [1–3]. When the geometry of the building structure in the environment is simulated as polygons for use in database, the diffraction and reflection points of each ray path will be determined via solutions of linear systems of planar geometries, and it makes the ray tracing codes run faster. However, when the objects could not be simulated as polygon, then the wave interaction would be complicated in terms of the diffraction/reflection points, and is resulted in different propagation mechanisms and contributed rays. In this case, algorithms must account for surface diffraction, for example creeping waves for convex surfaces and whispering gallery modes for concave surfaces, over curved structures as has been done in computation of radar cross section (RCS) of complex structures.

In this study, we attempt to provide insights on extending capability of ray tracing algorithms for modelling curved building structures in urban radio propagation as smooth convex surfaces [4, 5]. Section 2 describes urban radio propagation and in particular, structural shadowing aspects of urban radio environment. Section 3 describes modelling of buildings either as edge/wedge or convex geometrical shapes. A 3D model for a particular building composition involving curved geometries is studied in Section 4 that is followed by conclusions.

2. URBAN RADIO PROPAGATION

Geometrical and architectural features of buildings in short range urban radio propagation have been investigated recently [6–8]. One such urban scene is illustrated in Figure 1. Main processes in radio propagation, here, are considered to be reflection and diffraction in most of the ray tracing algorithms. For the cases when base
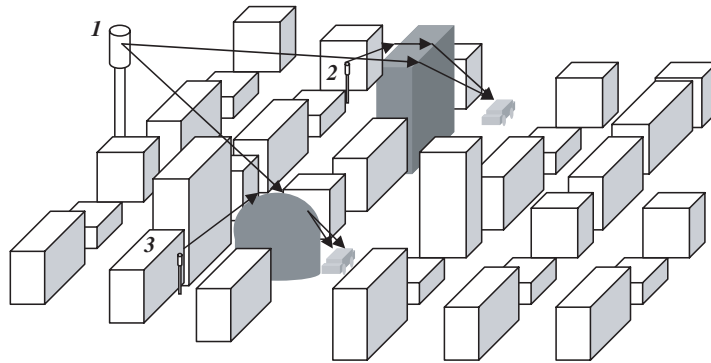
Figure 1. Radio propagation in urban environment (shadowing).

stations above rooftops (Tx-1), many statistical and deterministic radio propagation models have been proposed [1]. When both transmitter and receiver are below rooftop level (Tx-2), that seems to be the case in current and future wireless systems [9], there are two planes to be considered for ray paths; vertical and horizontal planes. Then, reflection and diffraction mechanism related to building structures in this case are considered to take place over polygons in both planes, and further these polygonal models can be simplified to have rectangular geometry. Either case simplifies the problem, and allows developing computationally fast tracing algorithms in calculating ray paths. Several ray tracing algorithms account for propagation over both planes for urban and rural areas [1, 10], such as three dimensional (3D) shooting and bouncing rays (SBR) that have also been used in RCS computation of large complex structures, vertical plane launch (VPL), and the 3D image method as discussed in [1], and in other radio propagation texts and survey papers.

In general, shadowing represents variations in mean path loss at a particular distance in urban radio propagation. In Figure 1, Tx-2 and Tx-3 would also represent two scenarios of shadowing due to buildings having different geometrical shapes, and also architectural features. Moreover, in higher transmitter positions labeled as Tx-1, the difference in the height of the buildings resulted in shadowing (variation in received signal strength or power). In lower transmitter positions, such as future systems targeting low transmission powers between peer to peer and/or in between relay nodes [9], single building structure having different geometries might individually cause shadowing loss. Both cases could be studied via ray tracing, and be modelled in order to integrate them in ray tracing algorithms. Analysis of shadowing effects
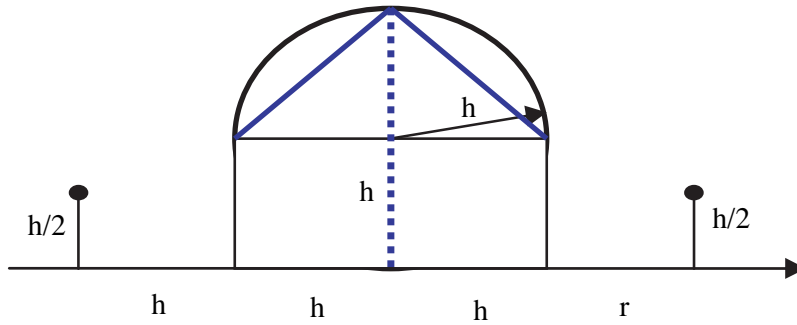
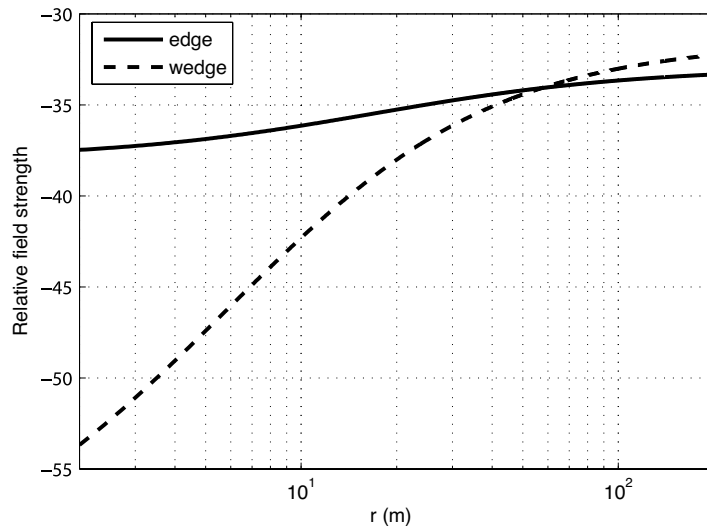**Figure 2a.** Edge/wedge and convex modelling of a building structure.

Figure 2b. Comparison of relative path loss for edge/wedge modelling.

are also considered to be important for short range indoor systems [11], and similar UTD analysis can be applied to estimate shadowing loss due to human body blockage in both indoor transmission and radio based position location systems.

Radio propagation models have initially focused on prediction of propagation loss for coverage. They usually modelled buildings as either knife edges or wedges [1] as illustrated in Figure 2. Later, they have been improved to include impedance wedge model to simulate mountains and hills. More recent attempts exploiting convex modelling

of hills and mountains along with wedge modelling of buildings in urban environment have been reported [12]. As the knowledge of the authors, none of the ray tracing algorithms for urban radio propagation has been able to model "curved building structures as smooth convex geometries". Such modelling would be important in prediction of shadowing loss as described in Figure 1 since the dominant mechanism in all three paths illustrated in Figure 1 involves shadowing due to building obstruction. For instance, the Tx-2 path represents a structure having non-polygonal geometry. This structure can be modelled approximately as edge or wedge, or a convex geometry when to be more realistic, which is naturally more accurate in prediction of shadowing loss via ray tracing techniques. In this case, the comparison of relative path loss as the receiver moves behind the structure in Figure 2(a) is shown in Figure 2(b) for edge and wedge modelling of the structure. Here, deep shadow region is more significant for propagation prediction, and convex modelling of structure has shown to produce path loss values much greater than that of an edge/wedge modelling as expected, and not shown in the plot. This is due to the fact that the radio waves travelling along the convex surface, the so-called creeping wave, attenuate much faster than a wave experiencing single point diffraction. In what follows, 3D modelling of a composition of structures having convex geometries will be considered. An analysis related to single and multiple diffractions effects without slope contribution [13] will studied via ray tracing technique on a particular scenario.

3. 3D MODELLING OF MULTIPLE NON-POLYGONAL STRUCTURES

As described in Section 2, most of the ray-tracing codes consider only vertical or horizontal planes for ray paths, and some of which can combine both planes in order to develop full 3D modelling of radio propagation [1, 14]. However, none of the ray-tracing codes developed so far for urban radio propagation are able take into account convex modelling of curved structures. This section aims to demonstrate modelling of non-polygonal structures in urban environments as canonical curved geometries, and study radio propagation over a particular building composition.

Consider the geometry shown in Figure 3 where an isolated cone-cylinder combination and hemisphere are placed symmetrically along the y axis. This is a typical geometry to model most of the mosques in the cities of Muslim countries including Turkey. The motivation in choosing this particular structure is that most cities have

somehow similar huge, non-planar building structures like cathetral, sport centers and churchs etc. A mosque is typically made of a minaret and a dome. In some big/medium-size mosques, there might be multiple minarets and domes. Here, one that could represent a small/medium size mosque is considered, and is assumed to have single minaret/dome pair. Figure 3 shows canonical geometries that would represent approximately a single minaret/dome pair. The minaret can be decomposed into a small angle cone and a cylinder on which the cone is placed. The dome is geometrically a hemisphere placed on a building of rectangular shape. The conical section of the minaret placed on a cylinder of radius is assumed to have a small apex angle of α. Detailed analysis of scattering from perfectly conducting cone is given in [15, 16] whose results are exploited in this study. The hemisphere representing the dome has a radius of r_s, and assumed to be placed on a rectangular building structure. In the analysis, since the motivation was to demonstrate that convex surface diffraction would be important, and can be integrated in modelling urban radio propagation, diffraction mechanisms at the junctions of cone-cylinder, sphere-rectangular structure all are ignored. Moreover, successive surface diffractions up to second order are considered in the analysis. As being different from conventional edge diffraction, tip diffraction due to the cone is also taken into account in the analysis.
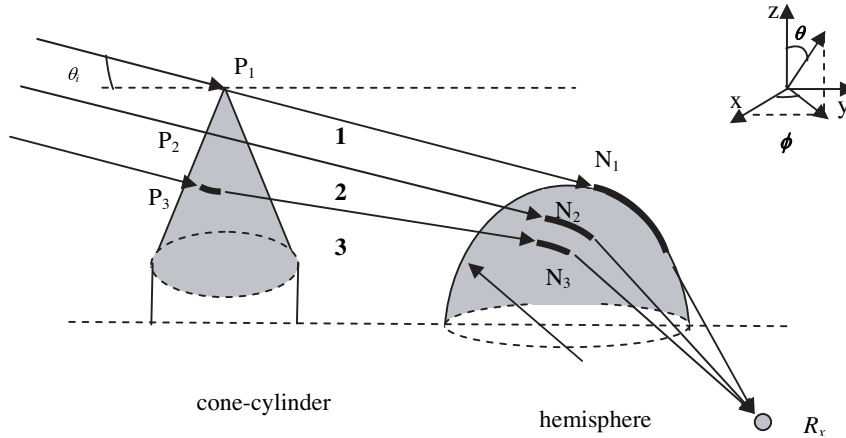

Figure 3. Illustration of 3D ray tracing for minaret-dome configuration.

In Figure 3, assume an incident plane wave of horizontal polarization ($\phi_i = \pi/2$) with an electric field given by

$$\overline{E}^i = \hat{\phi}e^{-jk\hat{s}\cdot\overline{r}}$$

where $\hat{s} = \hat{y}\sin\theta_i - \hat{z}\cos\theta_i$ and $\overline{r} = y\hat{y} + z\hat{z}$. Assume that the reference phase plane is at the tip of the cone.

The major rays contributing to the receiver located at the rear side of the hemisphere (R_x) are

1. Tip diffracted (cone) + surface diffracted(hemisphere)
2. Surface diffracted (hemisphere)
3. Surface diffracted (cone or cylinder) + surface diffracted (hemisphere).

P_3, N_1, N_2 and N_3 represent attachment poinst while P'_3, N'_1, N'_2 and N'_3 (not shown) represent shedding points for surface diffracted rays. According to the Fermat's principle [3], the path followed by the ray 1 should be an extremum. For homogenous medium, the trajectory of the ray 1 will be the composition of a) a straight line segment from P_1 to the attachment point N_1 b) the geodesic path segment from the attachment point N_1 to the shedding point N'_1 c) straight line segment from N'_1 to the receiving point R_x, all being on the $x = 0$ plane for plane wave incidence case.

The electric field due to ray 1 can be written [4, 5] as

$$E^1_\phi(R_x) = E^d_\phi(N'_1)T_s\left(\rho_1, |\overline{s}_1|, |\overline{s}'_1|, r_s\right)\frac{e^{-jk|\overline{s}'_1|}}{|\overline{s}'_1|} \tag{1}$$

where the tip-diffracted field is

$$E^d_\phi(N'_1) = E^i(P_1)\left(\frac{\alpha}{2}\right)^2 f(\theta_i, \theta_d)\frac{e^{-jk|\overline{s}_1|}}{jk|\overline{s}_1|} \tag{2}$$

where the incident electric field at the tip of the cone is $E^i(P_1)$, the diffraction pattern of the conical tip is $f(\theta_i, \theta_d)$ given [16], and is evaluated in [4, 5]. $\overline{s}_1$ is the vector from the tip of the cone to the attachment point N_1 on the hemisphere of radius r_s while $\overline{s}'_1$ is the vector from the shedding point N'_1 on the hemisphere to the receiving point R_x on the y-axis ($x = 0$ plane). The surface diffraction coefficient is $T_s(\rho_1, |\overline{s}_1|, |\overline{s}'_1|, r_s)$, where ρ_1 is the path length (arc) of the creeping wave. The surface diffraction coefficient is given by

$$T_s(\rho_1, |\overline{s}_1|, |\overline{s}'_1|, r_s) =$$
$$-\sqrt{m(N'_1)m(N_1)}\sqrt{\frac{2}{k}}e^{-jk\rho}\left\{\frac{e^{-j\pi/4}}{2\varsigma\sqrt{\pi}}[1 - F(x)] + \hat{P}_s(\varsigma)\right\} \tag{3}$$

where the radius of the curvature for the hemisphere is $m(N'_1) = m(N_1) = (kr_s/2)^{1/3}$, $x = kL\rho_1^2/2r_s^2$ and $\varsigma = \rho_1(k/2r_s^2)^{1/3}$ with a

radius of sphere r_s. $\hat{P}_s(\varsigma)$ is the Fock scattering function, and $F(x)$ is the Fresnel function. The computational aspects of the functions and other parameters can be found in [2–5].

Among the three rays, the second will be the dominant in contributing to the received signal strength since it subjects to single surface diffraction while all others have at least two successive diffractions. This ray passes just above the cone surface designated by P_2 in Figure 3, and attach the hemisphere at N_2, and travels along an arc of the length ρ_2, leaves the hemisphere at the shedding point N_2' in order to arrive at the receiver R_x. The electric field for the ray 2 has, then, two components given by

$$\begin{bmatrix} E_\theta^2(Rx) \\ E_\phi^2(Rx) \end{bmatrix} = E_\phi^i(N_2)T_s(\rho_2, |\overline{s}_2|, |\overline{s}_2'|, r_s) \begin{bmatrix} \sin\phi_p \\ \cos\phi_p \end{bmatrix} \frac{e^{-jk|\overline{s}_2'|}}{|\overline{s}_2'|}. \quad (4)$$

Here, the angle ϕ_p is measured on the xy plane according to the attachment point and the receiving point. Other parameters are determiined as in ray 1 with different diffracting points. The incident field at N_2 in (4) is written as

$$E_\phi^i(N_2) = E_\phi^i(0)e^{-jk}\left[(y_{N_2} - y_{P_2})\sin\theta_i + (z_{P_2} - z_{N_2})\cos\theta_i\right] \quad (5)$$

where $E_\phi^i(0)$ is the electric field at the reference phase plane.

The third ray first hits (P_3) either conical or cylindrical section of the minaret depending on the angle of incidence θ_i, departs (P_3') from the surface with an angle ϕ_3 in horizontal plane in order to arrive at the receiver, and then experience one more surface diffraction over the hemisphere (N_3, N_3') as illustrated in Figure 3. The electric field at the receiver due to the third ray is determined as

$$\begin{bmatrix} E_\theta^3(Rx) \\ E_\phi^3(Rx) \end{bmatrix} = \begin{bmatrix} -T_s & 0 \\ 0 & -T_h \end{bmatrix} \cdot \begin{bmatrix} E_\theta^3(N_3) \\ E_\phi^3(N_3) \end{bmatrix} \cdot \frac{e^{-jk|\overline{s}_{3d}'|}}{|\overline{s}_{3d}'|} \quad (6)$$

where $T_{s,h}$ is the surface diffraction coefficient for vertical and horizontal polarizations, the electric field before surface diffraction on the hemisphere is given by

$$\begin{bmatrix} E_\theta^3(N_3) \\ E_\phi^3(N_3) \end{bmatrix} = E_\phi^i(P_3) \cdot T_s(P_3, P_3', \rho_3, \overline{s}_3, \overline{s}_3') \begin{bmatrix} \sin\phi_3 \\ \cos\phi_3 \end{bmatrix} \frac{e^{-jk|\overline{s}_3'|}}{|\overline{s}_3'|} \quad (7)$$

Where again the surface diffraction coefficient is determined as in ray 1, with ρ_3 being the arc length of the creeping wave. All diffracting points above are computed numerically by solving linear systems of equations via numerical methods such as Newton-Raphson.

4. SHADOWING LOSS

The total field is obtained by summing all the ray components determined in Section 3. This would be either vector sum or power sum. While the phase of each ray is considered in vector sum, the only the power of each ray is considered in power sum. Here, the number of rays is only 3. It should be noted that the base station 1 (Tx1) illustrated in Figure 1 would resembles the scenario considered in the previous section. Then, shadowing loss described previously can be determined as relative path loss of the total electric field at the receiving point. In other words, the shadowing loss is, here, equivalent to the diffraction loss in the analysis. When power sum is used, the diffraction loss is given as

$$L_D = -10 \log \left[\sum_{n=1}^{N} \left| \overline{E}_n(Rx) \right|^2 \right] - 10 \log \left(\left| \overline{E}^i(Rx) \right|^2 \right) \qquad (8)$$

where the first term represents the sum of the contributing rays at the receiver point, and the second term represents free space field contribution (or path loss) when the structure is absent. The diffraction loss due to vector sum of the rays can also be determined, and is shown in Figure 4. Co-polar and cross polar components of each ray considered in Figure 3 is plotted in Figures 5(a) and (b). As expected, the dominant ray path will be ray 2 whose contribution at least, 30 dB above the nearest one.
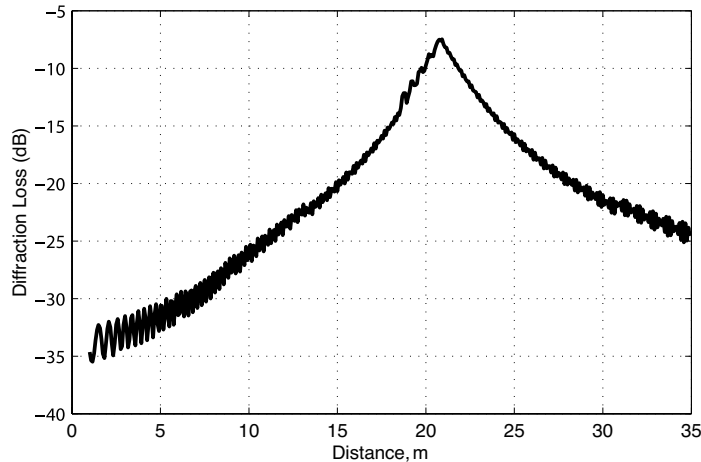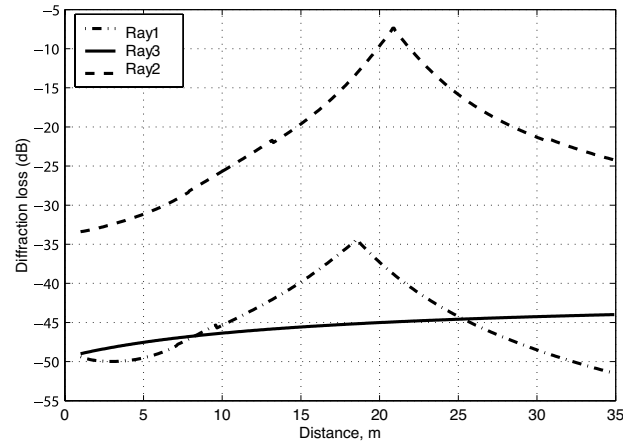

Figure 4. Relative diffraction loss.

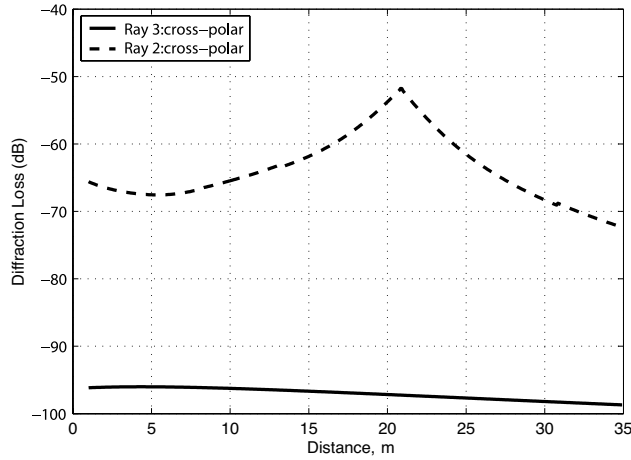**Figure 5a.** Contributing rays (co-polar components).

Figure 5b. Contributing rays (cross-polar components).

5. CONCLUSIONS

This paper has provided an insight on extending of ray tracing algorithm to model curved building structures as smooth convex structure. Shadowing loss due to a particular building composition, a minaret-dome composition representing a small/medium size mosque, in urban radio propagation has been determined via UTD ray tracing. Although 3D curved modelling provides more accurate modelling and

seems to be more realistic, it also brings about larger computation time due to the complexity introduced in calculating of diffraction points over convex geometries. In order to determine the dominant ray paths and diffraction points for the 3D building composition in the analysis, a system of equations (second order) involving up to six unknowns need to be solved numerically. In this particular case, the computation time is still reasonable, on the order of several tens of seconds for each simulation in MATLAB. However, when the mixed building structure is to be used in ray tracing algorithms for modeling complex urban radio propagation, there is still a trade off between accuracy and computation time.

REFERENCES

1. Bertoni, H. L., *Radio Propagation for Modern Wireless Systems*, Prentice Hall, 2000.
2. Pathak, H. P., W. D. Burnside, and R. J. Marhefka, "A uniform GTD analysis of the diffraction of electromagnetic waves by a smooth convex surface," *IEEE Trans. on Antennas and Prop.*, Vol. 28, No. 5, 631–642, 1980.
3. McNamara, D. A., C. W. I. Pistorious, and J. A. G. Malherbe, *Introduction to the Uniform Geometrical Theory of Diffraction*, Artech House, 1991.
4. Kara, A. and E. Yazgan, "Shadowing effects of huge non-rectangular structures in urban environments for wireless communications," *IV. International Workshop on Electromagnetic Wave Scattering (EWS'2006)*, 68–73, Gebze, Turkey, 2006.
5. Kara, A., "Theoretical and experimental investigation of radio propagation for urban and indoor wireless communication systems at UHF band," Ph.D. thesis, Hacettepe University, 2002.
6. Dimitriou, A. G. and G. D. Sergiadis, "Architectural features and urban propagation," *IEEE Trans. on Antennas and Prop.*, Vol. 54, No. 3, 774–784, 2006.
7. El-Sallabi, H., G. Liang, H. L. Bertoni, I. T. Rekanos, and P. Vainikainen, "Influence of diffraction coefficient and corner shape on ray prediction of power and delay spread in urban microcells," *IEEE Trans. on Antennas and Prop.*, Vol. 50, No. 5, 703–712, 2002.
8. Kara, A. and E. Yazgan, "Roof shape modelling for multiple diffraction loss in cellular mobile communication systems," *Int. Journal of Electronics*, Vol. 89, No. 10, 753–758, 2002.
9. Wang, Z., E. K. Tameh, and A. R. Nix, "Statistical peer-to peer

channel models for outdoor urban environments at 2 GHz and 5 GHz," *IEEE Veh. Tech. Conf.*, 5101–5105, 2006.

10. Lebherz, M., W. Wiesbeck, and W. Krank, "A versatile wave propagation model for the VHF/UHF range considering three-dimensional terrain," *IEEE Trans. on Antennas and Prop.*, Vol. 40, No. 10, 1121–1131, 1992.

11. Kara, A. and H. L. Bertoni, "Effect of people moving near short-range indoor propagation links at 2.45 GHz," *Journal of Communications and Networks*, Vol. 8, No. 3, 286–289, 2006.

12. Rodriguez, J. V., J. M. Molina-Garcia-Pardo, and L. Juan-Llacer, "A new solution for the analysis of multiple-building diffraction in urban areas with shadowing caused by a cylindrical hill," *IEEE Trans. on Antennas and Prop.*, Vol. 55, No. 19, 2632–2636, 2007.

13. Kara, A., H. L. Bertoni, and E. Yazgan, "Limit and application range of slope diffraction method for wireless communications," *IEEE Trans. on Antennas and Prop.*, Vol. 51, No. 9, 2512–2514, 2003.

14. Liang, G. and H. L. Bertoni, "A new approach to 3-D ray tracing for propagation prediction in cities," *IEEE Trans. on Antennas and Prop.*, Vol. 46, No. 6, 853–863, 1998.

15. Trott, K. D., P. H. Pathak, and F. A. Molinet, "A UTD type analysis of the plane wave scattering by a fully illuminated perfectly conducting cone," *IEEE Trans. on Antennas and Prop.*, Vol. 38, No. 8, 1150–1160, 1990.

16. Felsen, L. B., "Plane-wave scattering by small-angle cones," *IRE Trans. on Antennas and Prop.*, No. 5, 121–129, 1957.